

Study of the $B^- \rightarrow K^- \eta \eta_c$ decay due to the $D\bar{D}$ bound state

Xin-Qiang Li,^{1,2,*} Li-Juan Liu,^{3,†} En Wang,^{3,4,‡} and Le-Le Wei^{1,§}

¹*Institute of Particle Physics and Key Laboratory of Quark and Lepton Physics (MOE),
Central China Normal University, Wuhan, Hubei 430079, China*

²*Center for High Energy Physics, Peking University, Beijing 100871, China*

³*School of Physics and Laboratory of Zhongyuan Light,
Zhengzhou University, Zhengzhou, Henan 450001, China*

⁴*Guangxi Key Laboratory of Nuclear Physics and Nuclear Technology,
Guangxi Normal University, Guilin 541004, China*

We study the $B^- \rightarrow K^- \eta \eta_c$ decay by taking into account the S -wave contributions from the pseudoscalar meson–pseudoscalar meson interactions within the unitary coupled-channel approach, where the $D\bar{D}$ bound state is dynamically generated. In addition, the contribution from the intermediate resonance $K_0^*(1430)^-$, with $K_0^*(1430)^- \rightarrow K^- \eta$, is also considered. Our results show that there is a clear peak around 3720 MeV in the $\eta \eta_c$ invariant mass distribution, which could be associated with the $D\bar{D}$ bound state. The future precise measurements of the $B^- \rightarrow K^- \eta \eta_c$ process at the Belle II and LHCb experiments could be, therefore, used to check the existence of the $D\bar{D}$ bound state, and to deepen our understanding of the hadron-hadron interactions.

I. INTRODUCTION

Since the discovery of $X(3872)$ by the Belle Collaboration in 2003 [1], many exotic states, which do not fit into the expectations of conventional quark models, have been observed experimentally during the past two decades [2]. Many of these exotic states, especially the ones observed in the charmonium sector, are observed around the threshold of a pair of heavy hadrons; some of them, such as $X(3872)$ [3], $Z_c(3900)$ [4] and $X(4160)$ [5], can be explained as the hadronic molecules. However, the hadronic molecular states with mass near the $D\bar{D}$ threshold have not yet been observed experimentally, and further detailed studies are therefore required both theoretically and experimentally [6].

In Ref. [7], by taking into account the $\pi\pi$, $K\bar{K}$, $D\bar{D}$, $D_s\bar{D}_s$, $\eta\eta$, and $\eta\eta_c$ coupled channels, the authors predicted a narrow hidden charm resonance with quantum numbers $I(J^{PC}) = 0(0^{++})$ and mass around 3700 MeV, which will be denoted as $X(3700)$ throughout this paper, within the unitary coupled-channel approach. Furthermore, by considering the η_c as a pure $c\bar{c}$ state and the η - η' mixing, together with the same parameters as used in Ref. [7], the pole of the new $X(3700)$ state was predicted to be $\sqrt{s} = (3722 - i18)$ MeV within the unitary coupled-channel approach [8]. The mass of the $D\bar{D}$ bound state predicted by other different models is also basically around the $D\bar{D}$ threshold [9–16], and the theoretical studies of the experimentally measured processes $e^+e^- \rightarrow J/\psi D\bar{D}$ [17–19], $B^+ \rightarrow D^0 \bar{D}^0 K^+$ [20] and $\gamma\gamma \rightarrow D\bar{D}$ [21–24] all support the existence of such a $D\bar{D}$ bound state. Meanwhile, some processes like

$\psi(3770) \rightarrow \gamma X(3700) \rightarrow \gamma \eta \eta'$, $\psi(4040) \rightarrow \gamma X(3700) \rightarrow \gamma \eta \eta'$, $e^+e^- \rightarrow J/\psi X(3700) \rightarrow J/\psi \eta \eta'$ [25], $\psi(3770) \rightarrow \gamma D\bar{D}$ [26], $\Lambda_b \rightarrow \Lambda D\bar{D}$ [27], and $B^+ \rightarrow K^+ \eta \eta'$ [28] have also been suggested to search for the $D\bar{D}$ bound state. It is worth mentioning that the BESIII Collaboration has recently searched for the $X(3700)$ in the $\psi(3770) \rightarrow \gamma \eta \eta'$ decay for the first time, observing however no significant signals due to the low detection efficiencies of the photons [29].

Although the $D\bar{D}$ bound state $X(3700)$ couples mainly to the $D\bar{D}$ and $D_s\bar{D}_s$ channels, it is not easy to search for any signals of the state in these systems. This is due to the fact that, since its mass is a little bit lower than the $D\bar{D}$ threshold, the $X(3700)$ state would manifest itself as a near-threshold enhancement in the $D\bar{D}$ invariant mass distribution, which may be difficult to identify due to the low detection efficiencies near the threshold [27, 30]. On the other hand, the $X(3700)$ state has also a sizeable coupling to the $\eta \eta_c$ channel, as observed in Refs. [7, 8]. Since the $\eta \eta_c$ threshold is about 200 MeV lower than the predicted mass of $X(3700)$, one expects that, if the $D\bar{D}$ bound state exists, a clear peak near the $D\bar{D}$ threshold would appear in the $\eta \eta_c$ invariant mass distribution of some processes with large phase space.

As is well known, the three-body weak decays of the B mesons involve much more complicated dynamics than do the two-body decays and can, therefore, provide a wealth of information about the meson-meson interactions and the hadron resonances [31–35] (see *e.g.*, Ref. [36] for a recent review). For instance, the $B \rightarrow K + X/Y/Z$ decay is an ideal process to produce the charmonium-like hadronic molecular states [11, 37–40], and many exotic states have been observed experimentally through the B -meson weak decays during the past few years, such as $Z_{cs}(4000)$, $Z_{cs}(4220)$ [41] and $X(4140)$ [42, 43] in $B^+ \rightarrow J/\psi \phi K^+$, as well as $X_0(2900)$ and $X_1(2900)$ in $B^+ \rightarrow D^+ D^- K^+$ decay [44, 45]. In this paper, we propose to search for the $D\bar{D}$ bound state $X(3700)$ in the $B^- \rightarrow K^- \eta \eta_c$ decay. It is worth mentioning that

*Electronic address: xqli@mail.ccnu.edu.cn

†Electronic address: liulijuan@zzu.edu.cn

‡Electronic address: wangen@zzu.edu.cn

§Electronic address: llwei@mails.ccnu.edu.cn

the Belle Collaboration has already searched for the process in 2015 based on 772×10^6 $B\bar{B}$ pairs collected at the $\Upsilon(4S)$ resonance [46], but no significant signal of the $D\bar{D}$ bound state was observed due to insufficient statistics. However, the Belle II Collaboration will accumulate about 50 times the Belle dataset [47, 48], and is expected to make further precise measurements of the $B^- \rightarrow K^- \eta \eta_c$ decay, which will shed more light on the existence of the $D\bar{D}$ bound state in this process. In addition, the authors of Ref. [49] have suggested to search for the $D\bar{D}$ bound state in the $\eta \eta_c$ mass distribution of the $B^+ \rightarrow K^+ \eta \eta_c$ decay, and predicted the branching ratio of $\mathcal{B}(B^+ \rightarrow X_{q\bar{q}}(\rightarrow \eta_c \eta) K^+) = (0.9 \sim 6.7) \times 10^{-4}$.

In this paper, motivated by the observations made above, we will study the $B^- \rightarrow K^- \eta \eta_c$ decay by taking into account the pseudoscalar meson–pseudoscalar meson interactions within the chiral unitary approach, from where the $D\bar{D}$ bound state is generated dynamically. On the other hand, the $B^- \rightarrow K^- \eta \eta_c$ decay can also proceed through the subsequent decay of the intermediate resonance $K_0^*(1430)$, *i.e.* $K_0^*(1430) \rightarrow K \eta$, whose contribution will be considered in this paper too. We will demonstrate that, besides a peak of $K_0^*(1430)$ in the $K^- \eta$ invariant mass distribution, there is a clear peak around 3720 MeV in the $\eta \eta_c$ invariant mass distribution, which could be associated with the $D\bar{D}$ bound state. Therefore, future precise measurements of the $B^- \rightarrow K^- \eta \eta_c$ decay at the Belle II and LHCb experiments could be used to check the existence of the $D\bar{D}$ bound state, and to deepen our understanding of the hadron-hadron interactions.

This paper is organized as follows. In Sec. II, we will firstly introduce our formalism for the $B^- \rightarrow K^- \eta \eta_c$ decay. Our numerical results and discussions are then presented in Sec. III. In Sec. IV, we give our final conclusion.

II. FORMALISM

In analogy to the discussions made in Refs. [27, 50–52], the $B^- \rightarrow K^- \eta \eta_c$ decay proceeds via the following three steps: the weak decay, the hadronization, and the final-state interactions. Explicitly, the b quark of the B^- meson firstly decays into a c quark and a virtual W^- boson, and then the W^- boson turns into a $\bar{c}s$ pair. In order to give rise to the $K^- \eta \eta_c$ final state, the \bar{u} anti-quark of the initial B^- meson and the $\bar{c}s$ pair from the W^- subsequent decay have to hadronize together with the $\bar{q}q$ ($\equiv \bar{u}u + \bar{d}d + \bar{s}s$) created from the vacuum with the quantum numbers $J^{PC} = 0^{++}$. The relevant quark-level diagrams can be classified as the internal and external W^- emission mechanisms, as depicted in Figs. 1(a)–(b) and 1(c)–(d), respectively. Here we have neglected all the Cabbibo-Kobayashi-Maskawa (CKM) suppressed diagrams that are proportional to the CKM element V_{ub} .

The meson-meson systems formed by the hadroniza-

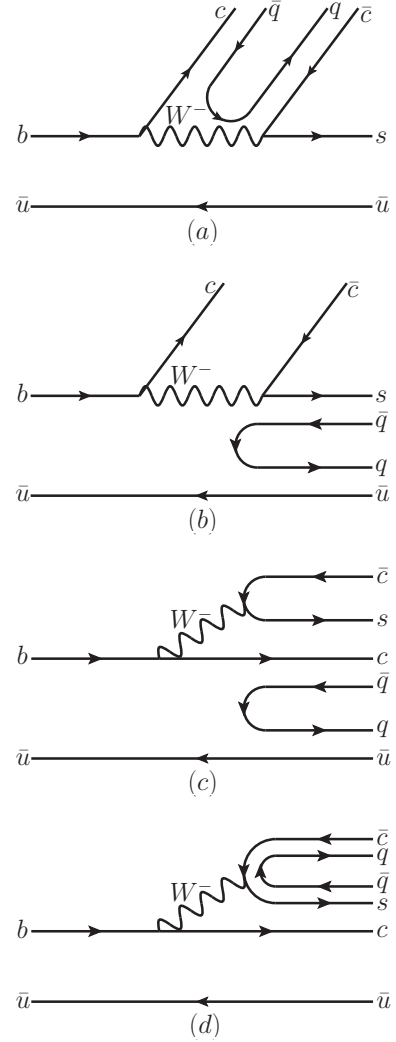


FIG. 1: The dominant quark-level diagrams for the $B^- \rightarrow K^- \eta \eta_c$ decay, where (a)–(b) and (c)–(d) refer to the internal and external W^- emission mechanisms, respectively.

tion of q_i , \bar{q}_j and $\bar{q}_k q_k$ are given by

$$\sum_{k=1}^3 q_i (\bar{q}_k q_k) \bar{q}_j = \sum_{k=1}^3 M_{ik} M_{kj} = (M^2)_{ij}, \quad (1)$$

with the $q\bar{q}$ matrix defined as

$$M = \begin{pmatrix} u\bar{u} & u\bar{d} & u\bar{s} & u\bar{c} \\ d\bar{u} & d\bar{d} & d\bar{s} & d\bar{c} \\ s\bar{u} & s\bar{d} & s\bar{s} & s\bar{c} \\ c\bar{u} & c\bar{d} & c\bar{s} & c\bar{c} \end{pmatrix}, \quad (2)$$

which could be expressed in terms of the physical pseu-

doscalar mesons as [33],

$$M = \begin{pmatrix} \frac{\eta}{\sqrt{3}} + \frac{\pi^0}{\sqrt{2}} + \frac{\eta'}{\sqrt{6}} & \pi^+ & K^+ & \bar{D}^0 \\ \pi^- & \frac{\eta}{\sqrt{3}} - \frac{\pi^0}{\sqrt{2}} + \frac{\eta'}{\sqrt{6}} & K^0 & D^- \\ K^- & \bar{K}^0 & \sqrt{\frac{2}{3}}\eta' - \frac{\eta}{\sqrt{3}} & D_s^- \\ D^0 & D^+ & D_s^+ & \eta_c \end{pmatrix}. \quad (3)$$

Thus, by isolating the meson K^- , one could easily obtain the components of the meson systems for Figs. 1(a) and 1(b) as follows:

$$\begin{aligned} |H\rangle^a &= V_p V_{cb} V_{cs}^* c(\bar{u}u + \bar{d}d + \bar{s}s)\bar{c}s\bar{u} \\ &= V_p V_{cb} V_{cs}^* (M^2)_{44} K^- \\ &= V_p V_{cb} V_{cs}^* \times (D^0 \bar{D}^0 + D^+ D^- + D_s^+ D_s^-) K^-, \end{aligned} \quad (4)$$

$$\begin{aligned} |H\rangle^b &= V_p V_{cb} V_{cs}^* c\bar{c}s(\bar{u}u + \bar{d}d + \bar{s}s)\bar{u} \\ &= V_p V_{cb} V_{cs}^* (M^2)_{31} \eta_c \\ &= V_p V_{cb} V_{cs}^* \times \left(\frac{1}{\sqrt{2}} K^- \pi^0 + \frac{3}{\sqrt{6}} K^- \eta' \right) \eta_c, \end{aligned} \quad (5)$$

where $V_{cb} = 0.04182$ and $V_{cs}^* = 0.97349$ are the CKM matrix elements, and V_p encodes all the remaining factors arising from the production vertex. Then, the final-state interactions of $D\bar{D}$, $D_s\bar{D}_s$, and $\eta'\eta_c$ will dynamically generate the $D\bar{D}$ bound state, which could decay into the $\eta\eta_c$ system. Here we do not consider the component $K^- \pi^0 \eta_c$, since the isospin of the $\pi^0 \eta_c$ system is $I = 1$.

Similarly, we can write the hadron components for Figs. 1(c) and 1(d) that could couple to the $K^- \eta \eta_c$ system as follows:

$$|H\rangle^c = V_p V_{cb} V_{cs}^* \times C \times (K^- D_s^+) D_s^-, \quad (6)$$

$$|H\rangle^d = V_p V_{cb} V_{cs}^* \times C \times (K^- \bar{D}^0) D^0, \quad (7)$$

where we have introduced the color factor C to account for the relative weight of the external W^- emission mechanism with respect to the internal W^- emission mechanism, and will take $C = 3$ in the case of color number $N_C = 3$, as done in Refs. [53–55].

According to the above discussions, the $K^- \eta \eta_c$ final state could not be produced directly through the tree-level diagrams of the B^- decay, but can via the final-state interactions of the coupled channels $D^0 \bar{D}^0$, $D^+ D^-$, $D_s^+ D_s^-$, and $\eta' \eta_c$, which could then generate the $D\bar{D}$ bound state, as shown in Fig. 2. The total amplitude of Fig. 2 can be expressed as

$$\begin{aligned} \mathcal{T}_X &= V_p V_{cb} V_{cs}^* \left[G_{D^+ D^-} t_{D^+ D^- \rightarrow \eta \eta_c} \right. \\ &\quad + (1 + C) \times G_{D^0 \bar{D}^0} t_{D^0 \bar{D}^0 \rightarrow \eta \eta_c} \\ &\quad + (1 + C) \times G_{D_s^+ D_s^-} t_{D_s^+ D_s^- \rightarrow \eta \eta_c} \\ &\quad \left. + \frac{3}{\sqrt{6}} \times G_{\eta' \eta_c} t_{\eta' \eta_c \rightarrow \eta \eta_c} \right], \end{aligned} \quad (8)$$

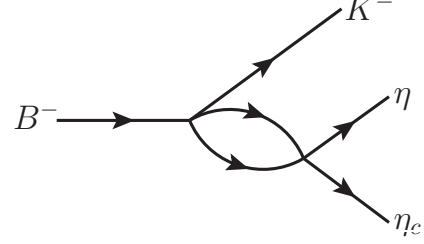


FIG. 2: The final-state interactions of the coupled channels $D^0 \bar{D}^0$, $D^+ D^-$, $D_s^+ D_s^-$, and $\eta' \eta_c$.

where G_l is the loop function for the two-meson propagation in the l -th channel, and its explicit expression is given by [7]

$$\begin{aligned} G_l &= i \int \frac{d^4 q}{(2\pi)^4} \frac{1}{q^2 - m_1^2 + i\epsilon} \frac{1}{(P - q)^2 - m_2^2 + i\epsilon} \\ &= \frac{1}{16\pi^2} \left[\alpha_l + \ln \frac{m_1^2}{\mu^2} + \frac{m_2^2 - m_1^2 + s}{2s} \ln \frac{m_2^2}{m_1^2} \right. \\ &\quad \left. + \frac{p}{\sqrt{s}} \times \left(\ln \frac{s - m_2^2 + m_1^2 + 2p\sqrt{s}}{-s + m_2^2 - m_1^2 + 2p\sqrt{s}} \right. \right. \\ &\quad \left. \left. + \ln \frac{s + m_2^2 - m_1^2 + 2p\sqrt{s}}{-s - m_2^2 + m_1^2 + 2p\sqrt{s}} \right) \right], \end{aligned} \quad (9)$$

with the subtraction constant $\alpha_l = -1.3$ for the coupled channels $D^+ D^-$, $D^0 \bar{D}^0$, $D_s^+ D_s^-$, and $\eta' \eta_c$, and $\mu = 1500$ MeV, being the same as used in Ref. [8]. $\sqrt{s} = M_{\eta\eta_c}$ is the invariant mass of the two mesons in the l -th channel, and m_1 and m_2 are the masses of these two mesons. P is the total four-momentum of the two mesons in the l -th channel, and p is the magnitude of the three-momentum of each meson in the meson-meson center of mass frame, with

$$p = \frac{\lambda^{1/2}(s, m_1^2, m_2^2)}{2\sqrt{s}}, \quad (10)$$

where $\lambda(x, y, z) = x^2 + y^2 + z^2 - 2xy - 2yz - 2zx$ is the Källén function. The transition amplitudes in Eq. (8) are obtained by solving the Bethe-Salpeter equation in coupled channels [7, 8],

$$t = [1 - VG]^{-1}V, \quad (11)$$

where the matrix V is the potential constructed at the tree level for each one of the possible channels. Here we take into account the channels of $\pi^+ \pi^-$, $\pi^0 \pi^0$, $K^+ K^-$, $K^0 \bar{K}^0$, $\eta\eta$, $\eta\eta_c$, $D^+ D^-$, $D^0 \bar{D}^0$, $D_s^+ D_s^-$, $\eta\eta'$, $\eta'\eta'$, as well as $\eta'\eta_c$, and present the transition potential V_{ij} in Table I of App. A.

On the other hand, the $B^- \rightarrow K^- \eta \eta_c$ decay could also proceed via the intermediate excited kaon mesons. According to the Dalitz plot shown in Fig. 3, one can see that only the well-established resonance $K_0^*(1430)$ could contribute to this process, since the $K_0^*(1430)$ couples to

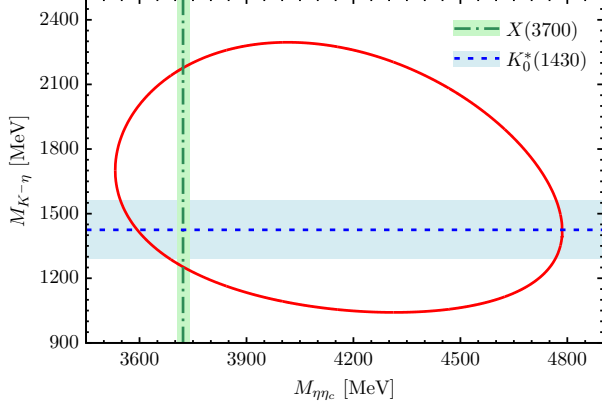


FIG. 3: The Dalitz plot for the $B^- \rightarrow K^- \eta \eta_c$ decay. The green dash-dotted line and band stand for the mass and width of $X(3700)$, while the blue dashed line and band for the mass and width of the well-established resonance $K_0^*(1430)$.

the channel $K^- \eta$ in S -wave with a branching fraction $\mathcal{B}(K_0^*(1430) \rightarrow K \eta) = (8.6_{-3.4}^{+2.7})\%$ [2]. Therefore, in this paper, we neglect all the other excited kaon mesons, and only take into account the contribution from the intermediate $K_0^*(1430)$ resonance as shown by Fig. 4, whose amplitude can be expressed as

$$\mathcal{T}_{K_0^*} = \frac{V_p \times \beta \times e^{i\varphi} \times M_{K_0^*(1430)}^2}{M_{K^- \eta}^2 - M_{K_0^*(1430)}^2 + i M_{K_0^*(1430)} \Gamma_{K_0^*(1430)}}, \quad (12)$$

where the parameter β accounts for the relative weight of the $K_0^*(1430)$ contribution with respect to that of the $D\bar{D}$ bound state $X(3700)$, and the phase factor $e^{i\varphi}$ is introduced to describe the interference between the amplitudes from the $D\bar{D}$ bound state and the $K_0^*(1430)$ resonance. $M_{K^- \eta}$ is the invariant mass of the $K^- \eta$ system. We will take as input $M_{K_0^*(1430)} = 1425$ MeV and $\Gamma_{K_0^*(1430)} = 270$ MeV [2].

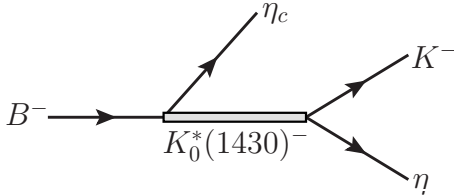


FIG. 4: The diagram for the $B^- \rightarrow K^- \eta \eta_c$ decay via the intermediate $K_0^*(1430)$ resonance.

With the amplitudes given by Eqs. (8) and (12) at hand, the doubly differential decay width of the $B^- \rightarrow$

$K^- \eta \eta_c$ process can be written as

$$\frac{d^2\Gamma}{dM_{\eta\eta_c} dM_{K^- \eta}} = \frac{1}{(2\pi)^3} \frac{M_{\eta\eta_c} M_{K^- \eta}}{8M_{B^-}^3} |\mathcal{T}_X + \mathcal{T}_{K_0^*}|^2 \quad (13)$$

$$\frac{d^2\Gamma}{dM_{\eta\eta_c} dM_{K^- \eta_c}} = \frac{1}{(2\pi)^3} \frac{M_{\eta\eta_c} M_{K^- \eta_c}}{8M_{B^-}^3} |\mathcal{T}_X + \mathcal{T}_{K_0^*}|^2 \quad (14)$$

One could obtain the invariant mass distributions $d\Gamma/dM_{\eta\eta_c}$, $d\Gamma/dM_{K^- \eta}$, and $d\Gamma/dM_{K^- \eta_c}$ by integrating Eqs. (13) and (14) over each of the invariant mass variables. For instance, the differential decay width $d\Gamma/dM_{\eta\eta_c}$ can then be obtained by integrating Eq. (13) over the $K^- \eta$ invariant mass $M_{K^- \eta}$, with the final result given by

$$\frac{d\Gamma}{dM_{\eta\eta_c}} = \int dM_{K^- \eta} \frac{1}{(2\pi)^3} \frac{M_{\eta\eta_c} M_{K^- \eta}}{8M_{B^-}^3} |\mathcal{T}_X + \mathcal{T}_{K_0^*}|^2. \quad (15)$$

Here the integration range is given by

$$\begin{aligned} & (M_{K^- \eta}^2)_{\min} \\ &= (E_{K^-}^* + E_{\eta}^*)^2 - \left(\sqrt{E_{\eta}^{*2} - m_{\eta}^2} + \sqrt{E_{K^-}^{*2} - m_{K^-}^2} \right)^2, \end{aligned} \quad (16)$$

$$\begin{aligned} & (M_{K^- \eta}^2)_{\max} \\ &= (E_{K^-}^* + E_{\eta}^*)^2 - \left(\sqrt{E_{\eta}^{*2} - m_{\eta}^2} - \sqrt{E_{K^-}^{*2} - m_{K^-}^2} \right)^2, \end{aligned} \quad (17)$$

where $E_{K^-}^*$ and E_{η}^* are the energies of K^- and η in the $\eta\eta_c$ rest frame, respectively. Explicitly, we have

$$E_{K^-}^* = \frac{M_{B^-}^2 - M_{\eta\eta_c}^2 - M_{K^-}^2}{2M_{\eta\eta_c}}, \quad (18)$$

$$E_{\eta}^* = \frac{M_{\eta\eta_c}^2 - M_{\eta_c}^2 + M_{\eta}^2}{2M_{\eta\eta_c}}. \quad (19)$$

Here all the meson masses involved are taken from Ref. [2].

III. RESULTS AND DISCUSSION

In our model, we have three free parameters, V_p , β and φ . The parameter V_p is a global factor and its value does not affect the shapes of the $\eta\eta_c$, $K^- \eta$, and $K^- \eta_c$ invariant mass distributions, and thus we take $V_p = 1$ for simplicity. The parameter β represents the relative weight of the $K_0^*(1430)$ contribution with respect to that of $X(3700)$, and the parameter φ is the relative phase between these two amplitudes.

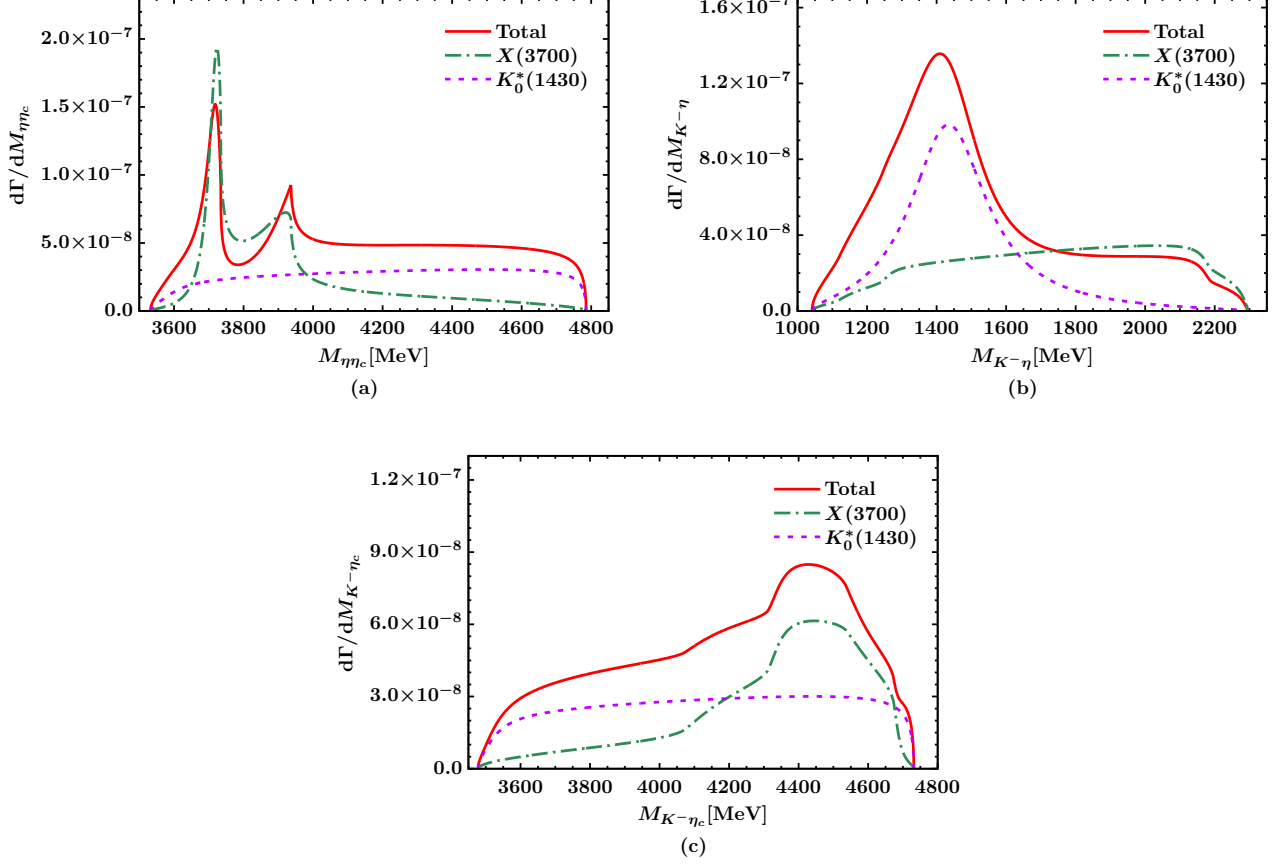


FIG. 5: The $\eta\eta_c$ (a), $K^-\eta$ (b) and $K^-\eta_c$ (c) invariant mass distributions of the $B^- \rightarrow K^-\eta\eta_c$ decay with $\beta = 0.012$, $\varphi = 0$ and $C = 3.0$. The green dash-dotted, the magenta dashed, and the red solid curves represent the contributions from $X(3700)$, $K_0^*(1430)$, and the total contributions, respectively.

As indicated by the current data on the branching fractions of B -meson decays [2],

$$\begin{aligned}\mathcal{B}(B^0 \rightarrow K_0^*(1430)^0 \eta_c) &= (1.8 \pm 0.4) \times 10^{-4}, \\ \mathcal{B}(B^0 \rightarrow K^0 D^+ D^-) &= (7.5 \pm 1.7) \times 10^{-4}, \\ \mathcal{B}(B^0 \rightarrow K^0 D^0 \bar{D}^0) &= (2.7 \pm 1.1) \times 10^{-4}, \\ \mathcal{B}(B^+ \rightarrow K^+ D^+ D^-) &= (2.2 \pm 0.7) \times 10^{-4}, \\ \mathcal{B}(B^+ \rightarrow K^+ D^0 \bar{D}^0) &= (1.45 \pm 0.33) \times 10^{-3},\end{aligned}$$

the branching fractions of the processes $B^0 \rightarrow K_0^*(1430)^0 \eta_c$ and $B^0 \rightarrow K^0 D \bar{D}$ are of the same order of magnitude. Thus, the contributions from the $D\bar{D}$ bound state and the $K_0^*(1430)$ resonance are expected to be of similar magnitudes. By integrating the differential decay width over the corresponding invariant mass, one can estimate the partial decay widths $\Gamma(B^- \rightarrow K_0^*(1430)^- \eta_c \rightarrow K^-\eta\eta_c)$ and $\Gamma(B^- \rightarrow K^- X(3700) \rightarrow K^-\eta\eta_c)$. It is found numerically that, with $\beta = 0.012$, the values of $\Gamma(B^- \rightarrow K_0^*(1430)^- \eta_c \rightarrow K^-\eta\eta_c)$ and $\Gamma(B^- \rightarrow K^- X(3700) \rightarrow K^-\eta\eta_c)$ are of the same order of magnitude. Therefore, in this work, we take the parameter $\beta = 0.012$ and also discuss our results with different values of β later.

Firstly, we show in Fig. 5 the $\eta\eta_c$, $K^-\eta$, and $K^-\eta_c$ invariant mass distributions with $\beta = 0.012$ and $\varphi = 0$. One can see a clear peak around 3720 MeV in the $\eta\eta_c$ invariant mass distribution, which should be associated with the $D\bar{D}$ bound state $X(3700)$. At the same time, a cusp structure appears around 3930 MeV in the same invariant mass distribution, which is due to the strong coupling of the $D\bar{D}$ bound state to the $D_s \bar{D}_s$ channel. In addition, a $K_0^*(1430)$ signal appears in the $K^-\eta$ invariant mass distribution, but gives rise to a smooth shape in the $\eta\eta_c$ invariant mass distribution and thus does not affect the peak structure of the $X(3700)$ significantly. It should be stressed that the line shape of the $X(3700)$ in the $\eta\eta_c$ invariant mass distribution is different from that of a Breit-Wigner form, which is a typical feature of the $D\bar{D}$ molecular state. On the other hand, one bump structure appears around 4400 MeV in the $K^-\eta_c$ invariant mass distribution, which is due to the $D\bar{D}$ interaction and hence should not be associated with any resonance.

It is worth mentioning that one narrow state $\chi_{c0}(3930)$, with mass around 3930 MeV and the quantum numbers $J^{PC} = 0^{++}$, was observed in the process $B^+ \rightarrow$

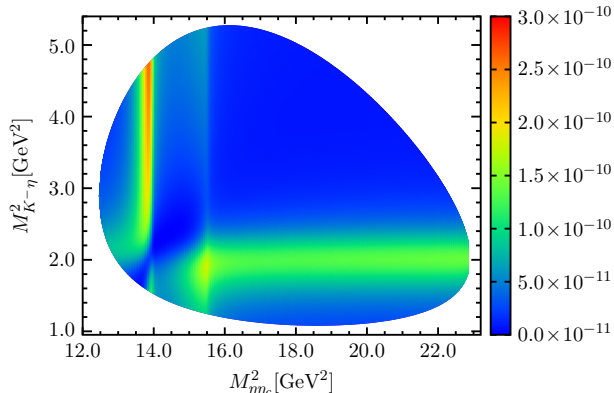


FIG. 6: The doubly differential decay width $d^2\Gamma / (dM_{\eta_c} dM_{K^- \eta})$ of the $B^- \rightarrow K^- \eta_c$ decay in the $(M_{\eta_c}^2, M_{K^- \eta}^2)$ plane, where the $X(3700)$ and $K_0^*(1430)$ resonances can be clearly seen.

$D^+ D^- K^+$ process by the LHCb Collaboration [45]. In addition, the LHCb Collaboration has discovered a peaking structure near the $D_s^+ D_s^-$ threshold, denoted as $X(3960)$ with $M = 3956 \pm 5 \pm 10$ MeV, $\Gamma = 43 \pm 13 \pm 8$ MeV and $J^{PC} = 0^{++}$, in the process $B^+ \rightarrow D_s^+ D_s^- K^+$ [56]. Some studies suggest that the near-threshold structure, $X(3960)$, may come from the $D_s^+ D_s^-$ bound state below the $D_s^+ D_s^-$ threshold, which can be associated with the $\chi_{c0}(3930)$ state [13, 57–64]. Taking into account the fact that the $\chi_{c0}(3930)$ and $X(3960)$ states favor the same quantum number $J^{PC} = 0^{++}$ and both of them can decay into the η_c final state, the cusp structure around 3930 MeV in the η_c invariant mass distribution could be associated with the resonance $X(3930)$. Therefore, the future precise measurements of this process could be used to search for the $\chi_{c0}(3930)$ and $X(3960)$ states.

We also show in Fig. 6 the doubly differential decay width $d^2\Gamma / (dM_{\eta_c} dM_{K^- \eta})$ for the $B^- \rightarrow K^- \eta_c$ decay in the $(M_{\eta_c}^2, M_{K^- \eta}^2)$ plane, where one can see two clear bands corresponding to the $X(3700)$ and $K_0^*(1430)$ resonances, respectively.

The parameters β and φ are unknown in our model, and their values could be determined if the precise experimental measurements of the $B^- \rightarrow K^- \eta_c$ decay are available in the future. In order to study the dependence of our results on β and φ , we have calculated the η_c , $K^- \eta$, and $K^- \eta_c$ invariant mass distributions with different values of β and φ , which are shown in Figs. 7 and 8, respectively. From Fig. 7, one can see that the peak of the $K_0^*(1430)$ resonance in the $K^- \eta$ invariant mass distribution becomes more significant when the value of β increases. From Fig. 8, on the other hand, the peak of $K_0^*(1430)$ moves a little bit for different values of φ . However, the peak of the $D\bar{D}$ bound state $X(3700)$ is always clear in the η_c invariant mass distribution.

Finally, we should note that the value of the color factor C , which represents the relative weight of the external W^- emission mechanism with respect to the internal W^- emission mechanism, could vary around 3 in order to account for the potential nonfactorizable contributions [65]. To this end, we show in Fig. 9 the η_c , $K^- \eta$, and $K^- \eta_c$ invariant mass distributions of the $B^- \rightarrow K^- \eta_c$ decay by taking three different values of $C = 3.0, 2.5, 2.0$. One can see that, although the peak of the $X(3700)$ state in the η_c invariant mass distribution becomes weaker when the value of C decreases, its signal is still clear and can be easily distinguished from the background contribution. Meanwhile, the peak of the $K_0^*(1430)$ resonance in the $K^- \eta$ invariant mass distribution has little changes for these three different values of C , because the contribution from the $D\bar{D}$ bound state is smooth around the peak of $K_0^*(1430)$ in the $K^- \eta$ invariant mass distribution, as observed already in Fig. 5.

From the above analyses, one can conclude that, within the variation ranges of the three free parameters, there is always a clear peak around 3720 MeV in the η_c invariant mass distribution, which corresponds to the $D\bar{D}$ bound state. Thus, we strongly suggest our experimental colleagues to perform more precise measurements of the $B^- \rightarrow K^- \eta_c$ decay at the Belle II and LHCb experiments in the future, which is very important for confirming the existence of the predicted $D\bar{D}$ bound state.

IV. CONCLUSIONS

In this paper, motivated by the theoretical predictions for the $D\bar{D}$ bound state $X(3700)$, we propose to search for this state in the $B^- \rightarrow K^- \eta_c$ decay. To this end, we have investigated the process within the unitary coupled-channel approach, by taking into account the contributions from the S -wave pseudoscalar meson–pseudoscalar meson interactions, which can dynamically generate the $D\bar{D}$ bound state $X(3700)$. We have also taken into account the contribution from the intermediate resonance $K_0^*(1430)$, since it couples to the $K\eta$ channel in S wave with a branching fraction of $\mathcal{B}(K_0^*(1430) \rightarrow K\eta) = (8.6_{-3.4}^{+2.7})\%$.

Our results show that a clear peak appears around 3720 MeV in the η_c invariant mass distribution, which should be associated with the $D\bar{D}$ bound state. It should be stressed that the line shape of the $D\bar{D}$ bound state is significantly different from that of a Breit-Wigner form, which is a typical feature of the $D\bar{D}$ molecular state. On the other hand, one can also find the peak of the resonance $K_0^*(1430)$ in the $K^- \eta$ invariant mass distribution, and the resonance gives a smooth contribution in the η_c invariant mass distribution.

In summary, we strongly encourage our experimental colleagues to perform a more precise measurement of the $B^- \rightarrow K^- \eta_c$ decay at the Belle II and LHCb experiments in the future, which will be very helpful to confirm the existence of the predicted $D\bar{D}$ bound state, as well

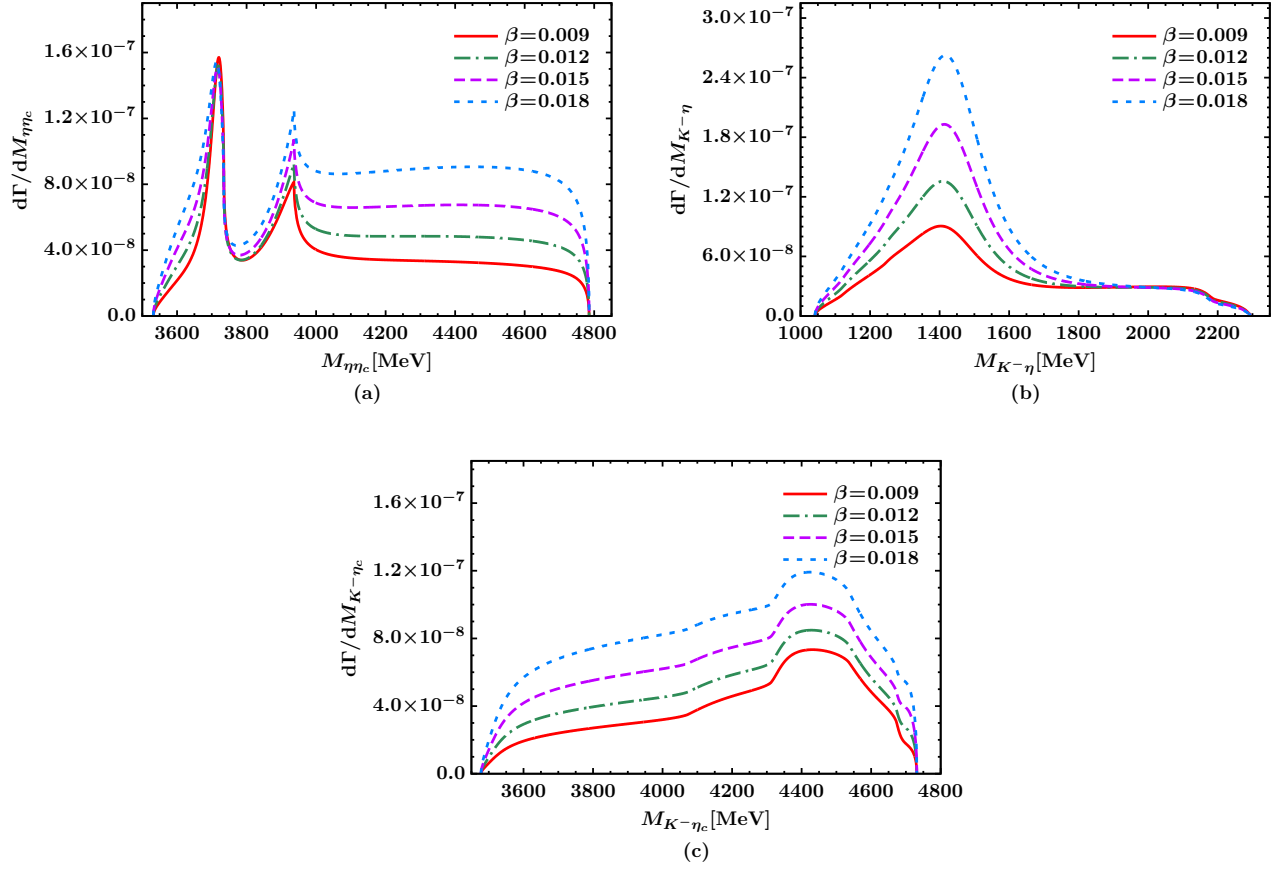


FIG. 7: The $\eta\eta_c$ (a), $K^-\eta$ (b) and $K^-\eta_c$ (c) invariant mass distributions of the $B^- \rightarrow K^-\eta\eta_c$ decay with $\varphi = 0$, $C = 3.0$, as well as four different values of $\beta = 0.009$ (red solid), 0.012 (green dash-dotted), 0.015 (magenta long-dashed) and 0.018 (blue dashed).

as to deepen our understanding of the hadron-hadron interactions.

Acknowledgements

This work is supported by the Natural Science Foundation of Henan under Grant No. 222300420554 and No. 232300421140, the National Natural Science Foundation of China under Grant No. 12135006, No. 12075097, and No. 12192263, the Project of Youth Backbone Teachers of Colleges and Universities of Henan Province (2020GGJS017), the Open Project of Guangxi Key Laboratory of Nuclear Physics and Nuclear Technology (No. NLK2021-08), as well as the Fundamental Research Funds for the Central Universities under Grant Nos. CCNU19TD012 and CCNU22LJ004.

Appendix A: Detailed derivations of the potential V

Following Refs. [7, 8], we can write the interaction Lagrangian as

$$\mathcal{L}_{\text{int}} = \frac{1}{12f^2} \text{Tr} [J_\mu J^\mu + \mathcal{M} \Phi^4], \quad (\text{A1})$$

where the current J^μ is defined by

$$J^\mu = (\partial^\mu \Phi) \Phi - \Phi (\partial^\mu \Phi), \quad (\text{A2})$$

and the matrix \mathcal{M} of the mass term reads

$$\mathcal{M} = \begin{pmatrix} m_\pi^2 & 0 & 0 & 0 \\ 0 & m_\pi^2 & 0 & 0 \\ 0 & 0 & 2m_K^2 - m_\pi^2 & 0 \\ 0 & 0 & 0 & 2m_D^2 - m_\pi^2 \end{pmatrix}. \quad (\text{A3})$$

In the physical basis, the matrix Φ can be written as [8]

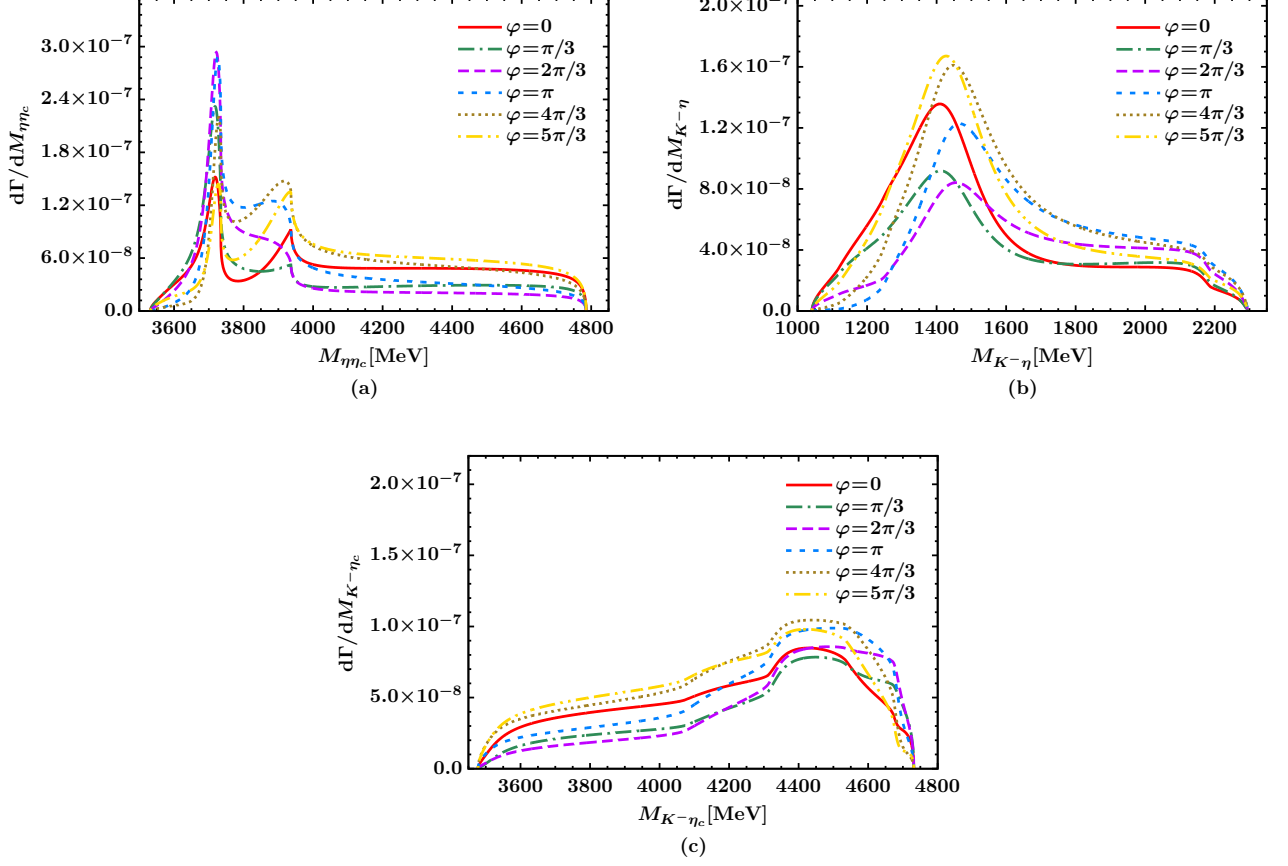


FIG. 8: The $\eta\eta_c$ (a), $K^-\eta$ (b) and $K^-\eta_c$ (c) invariant mass distributions of the $B^- \rightarrow K^-\eta\eta_c$ decay with $\beta = 0.012$, $C = 3.0$, as well as six different values of $\varphi = 0$ (red solid), $\pi/3$ (green dash-dotted), $2\pi/3$ (magenta long-dashed), π (blue dashed), $4\pi/3$ (olive dotted) and $5\pi/3$ (yellow dash-dot-dotted).

$$\Phi = \begin{pmatrix} \frac{\pi^0}{\sqrt{2}} + \frac{\eta}{\sqrt{3}} + \frac{\eta'}{\sqrt{6}} & \pi^+ & K^+ & \bar{D}^0 \\ \pi^- & \frac{\eta}{\sqrt{3}} - \frac{\pi^0}{\sqrt{2}} + \frac{\eta'}{\sqrt{6}} & K^0 & D^- \\ K^- & \bar{K}^0 & \sqrt{\frac{2}{3}}\eta' - \frac{\eta}{\sqrt{3}} & D_s^- \\ D^0 & D^+ & D_s^+ & \eta_c \end{pmatrix}. \quad (\text{A4})$$

which can be further decomposed into

$$\phi_8 = \begin{pmatrix} \frac{\pi^0}{\sqrt{2}} + \frac{\eta}{\sqrt{3}} + \frac{\eta'}{\sqrt{6}} & \pi^+ & K^+ \\ \pi^- & -\frac{\pi^0}{\sqrt{2}} + \frac{\eta}{\sqrt{3}} + \frac{\eta'}{\sqrt{6}} & K^0 \\ K^- & \bar{K}^0 & -\frac{\eta}{\sqrt{3}} + \sqrt{\frac{2}{3}}\eta' \end{pmatrix}, \quad (\text{A5})$$

$$\phi_{\bar{3}} = (D^0 \ D^+ \ D_s^+), \quad (\text{A6})$$

$$\phi_3 = \begin{pmatrix} \bar{D}^0 \\ D^- \\ D_s^- \end{pmatrix}, \quad (\text{A7})$$

$$\phi_1 = \eta_c. \quad (\text{A8})$$

Since the SU(4) flavor symmetry breaking already arises from the mass term \mathcal{M} , which is not proportional to the identity matrix [8], we are going to use the meson decay constant $f = f_\pi = 93$ MeV for light mesons, and $f = f_D = 165$ MeV for heavy ones. In addition, we are going to suppress all the terms in the Lagrangian where the interaction is driven by the exchange of a heavy

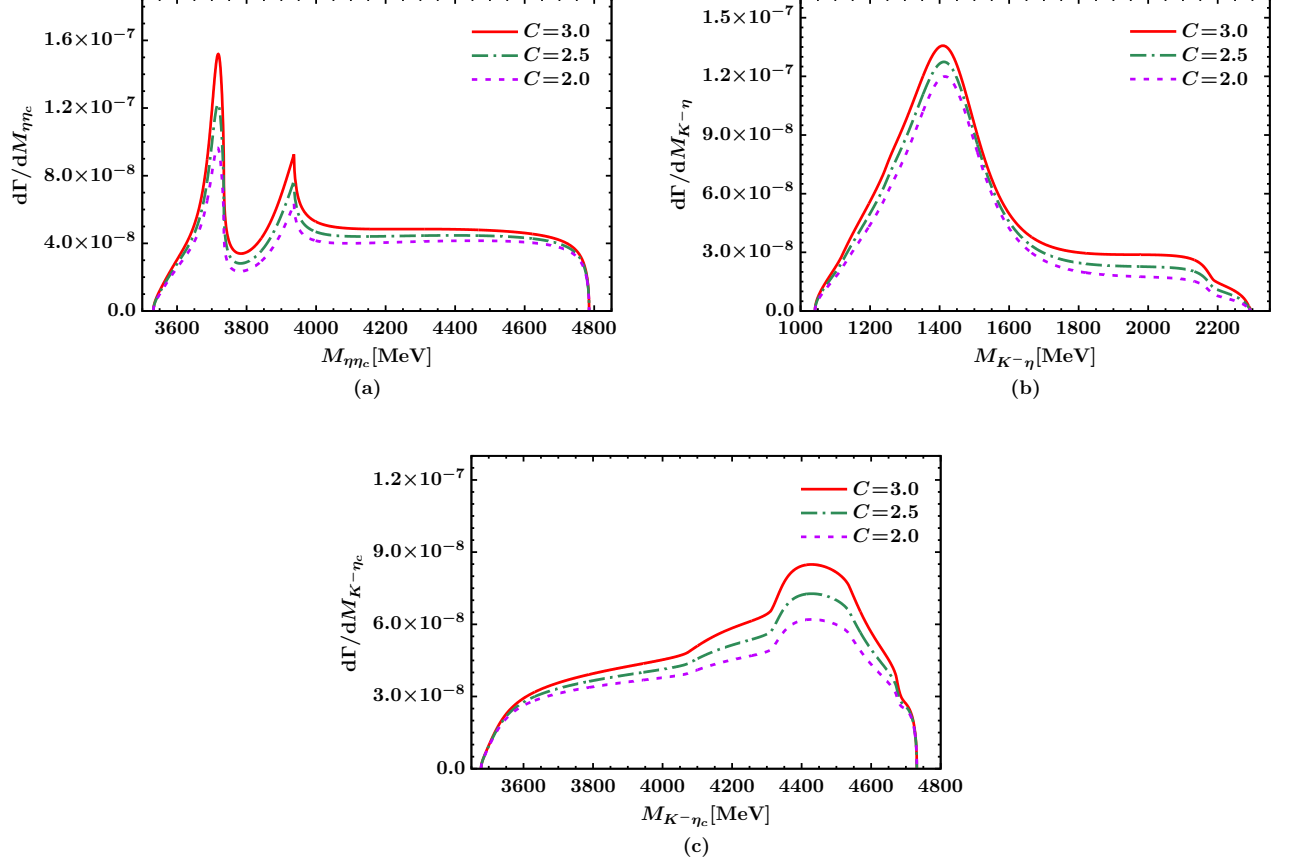


FIG. 9: The $\eta\eta_c$ (a), $K^-\eta$ (b) and $K^-\eta_c$ (c) invariant mass distributions of the $B^- \rightarrow K^-\eta\eta_c$ decay with $\beta = 0.012$, $\varphi = 0$, as well as three different values of $C = 3.0$ (red solid), 2.5 (green dash-dotted), and 2.0 (magenta dashed).

vector meson, as usually discussed in the vector meson dominance picture. For details of this suppression, one

could refer to Refs. [7? ? ?]. Finally, the full corrected Lagrangian can be written as,

$$\mathcal{L} = \frac{1}{12f^2} \left\{ \text{Tr} \left[J_{88\mu} J_{88}^\mu + 2J_{3\bar{3}\mu} J_{88}^\mu + J_{3\bar{3}\mu} J_{3\bar{3}}^\mu \right] + \frac{8}{3} \gamma J_{\bar{3}1\mu} J_{13}^\mu \right. \\ \left. + \frac{4}{\sqrt{3}} \gamma (J_{\bar{3}1\mu} J_{83}^\mu + J_{\bar{3}8\mu} J_{13}^\mu) + 2\gamma J_{\bar{3}8\mu} J_{83}^\mu + \psi_5 J_{\bar{3}3\mu} J_{33}^\mu + \mathcal{L}_{\text{mass}} \right\}, \quad (\text{A9})$$

with

and the correction parameters given by

$$\gamma = \left(\frac{m_L}{m_H} \right)^2, \quad (\text{A11})$$

$$\psi_3 = \frac{1}{3} + \frac{2}{3} \left(\frac{m_L}{m_{J/\psi}} \right)^2, \quad (\text{A12})$$

$$\psi_5 = -\frac{1}{3} + \frac{4}{3} \left(\frac{m_L}{m_{J/\psi}} \right)^2. \quad (\text{A13})$$

$$\mathcal{L}_{\text{mass}} = \text{Tr} [\mathcal{M}\Phi^4], \quad (\text{A10}) \quad \text{Here, } m_L \text{ and } m_H \text{ are the masses of light and heavy}$$

vector mesons respectively, and they will be set to $m_L = 800$ MeV and $m_H = 2050$ MeV [7]. When inserting these amplitudes in the Bethe-Salpeter equation, we should divide the amplitude by $1/\sqrt{2}$ each time when the initial or the final state contains a pair of identical particles (unitary normalization) in order to ensure closure of the

intermediate states.

In this paper, we take into account the coupled channels $\pi^+\pi^-$, $\pi^0\pi^0$, K^+K^- , $K^0\bar{K}^0$, $\eta\eta$, $\eta\eta_c$, D^+D^- , $D^0\bar{D}^0$, $D_s^+D_s^-$, $\eta\eta'$, $\eta'\eta'$, and $\eta'\eta_c$, and present the transition potential V_{ij} in Table I.

TABLE I: The transition potentials V_{ij} among different channels, where s , t and u are the Mandelstam variables.

Channel	Potential
$\pi^+\pi^- \rightarrow \pi^+\pi^-$	$-\frac{1}{3f^2} ((s+t-2u) + 2m_\pi^2)$
$\pi^+\pi^- \rightarrow \pi^0\pi^0$	$-\frac{1}{3f^2} ((2s-t-u) + m_\pi^2)$
$\pi^+\pi^- \rightarrow K^+K^-$	$-\frac{1}{6f^2} ((s+t-2u) + m_K^2 + m_\pi^2)$
$\pi^+\pi^- \rightarrow K^0\bar{K}^0$	$-\frac{1}{6f^2} ((s+u-2t) + m_K^2 + m_\pi^2)$
$\pi^+\pi^- \rightarrow \eta\eta$	$-\frac{2}{3f^2} m_\pi^2$
$\pi^+\pi^- \rightarrow \eta\eta_c$	0
$\pi^+\pi^- \rightarrow D^+D^-$	$-\frac{1}{6f^2} ((t-u) + \gamma(s-u) + m_D^2 + m_\pi^2)$
$\pi^+\pi^- \rightarrow D^0\bar{D}^0$	$-\frac{1}{6f^2} ((u-t) + \gamma(s-t) + m_D^2 + m_\pi^2)$
$\pi^+\pi^- \rightarrow D_s^+D_s^-$	0
$\pi^+\pi^- \rightarrow \eta\eta'$	$-\frac{\sqrt{2}}{3f^2} m_\pi^2$
$\pi^+\pi^- \rightarrow \eta'\eta'$	$-\frac{1}{3f^2} m_\pi^2$
$\pi^+\pi^- \rightarrow \eta'\eta_c$	0
$\pi^0\pi^0 \rightarrow \pi^0\pi^0$	$-\frac{1}{f^2} m_\pi^2$
$\pi^0\pi^0 \rightarrow K^+K^-$	$-\frac{1}{12f^2} ((2s-t-u) + 2m_K^2 + 2m_\pi^2)$
$\pi^0\pi^0 \rightarrow K^0\bar{K}^0$	$-\frac{1}{12f^2} ((2s-t-u) + 2m_K^2 + 2m_\pi^2)$
$\pi^0\pi^0 \rightarrow \eta\eta$	$-\frac{2}{3f^2} m_\pi^2$
$\pi^0\pi^0 \rightarrow \eta\eta_c$	0
$\pi^0\pi^0 \rightarrow D^+D^-$	$-\frac{1}{12f^2} (\gamma(2s-t-u) + 2m_D^2 + 2m_\pi^2)$
$\pi^0\pi^0 \rightarrow D^0\bar{D}^0$	$-\frac{1}{12f^2} (\gamma(2s-t-u) + 2m_D^2 + 2m_\pi^2)$
$\pi^0\pi^0 \rightarrow D_s^+D_s^-$	0
$\pi^0\pi^0 \rightarrow \eta\eta'$	$-\frac{\sqrt{2}}{3f^2} m_\pi^2$
$\pi^0\pi^0 \rightarrow \eta'\eta'$	$-\frac{1}{3f^2} m_\pi^2$
$\pi^0\pi^0 \rightarrow \eta'\eta_c$	0
$K^+K^- \rightarrow K^+K^-$	$-\frac{1}{3f^2} ((s+t-2u) + 2m_K^2)$
$K^+K^- \rightarrow K^0\bar{K}^0$	$-\frac{1}{6f^2} ((s+t-2u) + 2m_K^2)$
$K^+K^- \rightarrow \eta\eta$	$-\frac{2}{9f^2} ((2s-t-u) + m_K^2)$
$K^+K^- \rightarrow \eta\eta_c$	0
$K^+K^- \rightarrow D^+D^-$	0
$K^+K^- \rightarrow D^0\bar{D}^0$	$-\frac{1}{6f^2} ((u-t) + \gamma(s-t) + m_D^2 + m_K^2)$
$K^+K^- \rightarrow D_s^+D_s^-$	$-\frac{1}{6f^2} ((t-u) + \gamma(s-u) + m_D^2 + 2m_K^2 - m_\pi^2)$
$K^+K^- \rightarrow \eta\eta'$	$\frac{\sqrt{2}}{18f^2} ((2s-t-u) + 4m_K^2 - 3m_\pi^2)$

continued on next page

- continued from previous page

Channel	Potential
$K^+ K^- \rightarrow \eta' \eta'$	$-\frac{1}{36f^2} ((2s - t - u) + 34m_K^2 - 6m_\pi^2)$
$K^+ K^- \rightarrow \eta' \eta_c$	0
$K^0 \bar{K}^0 \rightarrow K^0 \bar{K}^0$	$-\frac{1}{3f^2} ((s + t - 2u) + 2m_K^2)$
$K^0 \bar{K}^0 \rightarrow \eta \eta$	$-\frac{2}{9f^2} ((2s - t - u) + m_K^2)$
$K^0 \bar{K}^0 \rightarrow \eta \eta_c$	0
$K^0 \bar{K}^0 \rightarrow D^+ D^-$	$-\frac{1}{6f^2} ((u - t) + \gamma(s - t) + m_D^2 + m_K^2)$
$K^0 \bar{K}^0 \rightarrow D^0 \bar{D}^0$	0
$K^0 \bar{K}^0 \rightarrow D_s^+ D_s^-$	$-\frac{1}{6f^2} ((t - u) + \gamma(s - u) + m_D^2 + 2m_K^2 - m_\pi^2)$
$K^0 \bar{K}^0 \rightarrow \eta \eta'$	$\frac{\sqrt{2}}{18f^2} ((2s - t - u) + 4m_K^2 - 3m_\pi^2)$
$K^0 \bar{K}^0 \rightarrow \eta' \eta'$	$-\frac{1}{36f^2} ((2s - t - u) + 34m_K^2 - 6m_\pi^2)$
$K^0 \bar{K}^0 \rightarrow \eta' \eta_c$	0
$\eta \eta \rightarrow \eta \eta$	$-\frac{2}{9f^2} (2m_K^2 + m_\pi^2)$
$\eta \eta \rightarrow \eta \eta_c$	0
$\eta \eta \rightarrow D^+ D^-$	$-\frac{1}{18f^2} (\gamma(2s - t - u) + 2m_D^2 + 2m_\pi^2)$
$\eta \eta \rightarrow D^0 \bar{D}^0$	$-\frac{1}{18f^2} (\gamma(2s - t - u) + 2m_D^2 + 2m_\pi^2)$
$\eta \eta \rightarrow D_s^+ D_s^-$	$-\frac{1}{18f^2} (\gamma(2s - t - u) + 2m_D^2 + 6m_K^2 - 4m_\pi^2)$
$\eta \eta \rightarrow \eta \eta'$	$\frac{4\sqrt{2}}{9f^2} (m_K^2 - m_\pi^2)$
$\eta \eta \rightarrow \eta' \eta'$	$-\frac{2}{9f^2} (4m_K^2 - m_\pi^2)$
$\eta \eta \rightarrow \eta' \eta_c$	0
$\eta \eta_c \rightarrow \eta \eta_c$	0
$\eta \eta_c \rightarrow D^+ D^-$	$-\frac{1}{3\sqrt{3}f^2} \left(\frac{1}{\sqrt{3}} \gamma(2s - t - u) + m_D^2 \right)$
$\eta \eta_c \rightarrow D^0 \bar{D}^0$	$-\frac{1}{3\sqrt{3}f^2} \left(\frac{1}{\sqrt{3}} \gamma(2s - t - u) + m_D^2 \right)$
$\eta \eta_c \rightarrow D_s^+ D_s^-$	$-\frac{1}{3\sqrt{3}f^2} \left(\frac{1}{\sqrt{3}} \gamma(t + u - 2s) - m_D^2 - m_K^2 + m_\pi^2 \right)$
$\eta \eta_c \rightarrow \eta \eta'$	0
$\eta \eta_c \rightarrow \eta' \eta'$	0
$\eta \eta_c \rightarrow \eta' \eta_c$	0
$D^+ D^- \rightarrow D^+ D^-$	$-\frac{1}{3f^2} (\psi_3(s + t - 2u) + 2m_D^2)$
$D^+ D^- \rightarrow D^0 \bar{D}^0$	$-\frac{1}{6f^2} (\psi_5(t - u) + (s - u) + 2m_D^2)$
$D^+ D^- \rightarrow D_s^+ D_s^-$	$-\frac{1}{6f^2} (\psi_5(t - u) + (s - u) + 2m_D^2 + m_K^2 - m_\pi^2)$
$D^+ D^- \rightarrow \eta \eta'$	$-\frac{\sqrt{2}}{36f^2} (\gamma(2s - t - u) + 2m_D^2 + 2m_\pi^2)$
$D^+ D^- \rightarrow \eta' \eta'$	$-\frac{1}{36f^2} (\gamma(2s - t - u) + 2m_D^2 + 2m_\pi^2)$
$D^+ D^- \rightarrow \eta' \eta_c$	$-\frac{1}{3\sqrt{6}f^2} \left(\frac{1}{\sqrt{3}} \gamma(2s - t - u) + m_D^2 \right)$
$D^0 \bar{D}^0 \rightarrow D^0 \bar{D}^0$	$-\frac{1}{3f^2} (\psi_3(s + t - 2u) + 2m_D^2)$
$D^0 \bar{D}^0 \rightarrow D_s^+ D_s^-$	$-\frac{1}{6f^2} (\psi_5(t - u) + (s - u) + 2m_D^2 + m_K^2 - m_\pi^2)$

continued on next page

- continued from previous page

Channel	Potential
$D^0 \bar{D}^0 \rightarrow \eta \eta'$	$-\frac{\sqrt{2}}{36f^2} (\gamma(2s - t - u) + 2m_D^2 + 2m_\pi^2)$
$D^0 \bar{D}^0 \rightarrow \eta' \eta'$	$-\frac{1}{36f^2} (\gamma(2s - t - u) + 2m_D^2 + 2m_\pi^2)$
$D^0 \bar{D}^0 \rightarrow \eta' \eta_c$	$-\frac{1}{3\sqrt{6}f^2} \left(\frac{1}{\sqrt{3}} \gamma(2s - t - u) + m_D^2 \right)$
$D_s^+ D_s^- \rightarrow D_s^+ D_s^-$	$-\frac{1}{3f^2} (\psi_3(s + t - 2u) + 2m_D^2 + 2m_K^2 - 2m_\pi^2)$
$D_s^+ D_s^- \rightarrow \eta \eta'$	$\frac{\sqrt{2}}{18f^2} (\gamma(2s - t - u) + 2m_D^2 + 6m_K^2 - 4m_\pi^2)$
$D_s^+ D_s^- \rightarrow \eta' \eta'$	$-\frac{1}{9f^2} (\gamma(2s - t - u) + 2m_D^2 + 6m_K^2 - 4m_\pi^2)$
$D_s^+ D_s^- \rightarrow \eta' \eta_c$	$-\frac{2}{3\sqrt{6}f^2} \left(\frac{1}{\sqrt{3}} \gamma(2s - t - u) + m_D^2 + m_K^2 - m_\pi^2 \right)$
$\eta \eta' \rightarrow \eta \eta'$	$-\frac{2}{9f^2} (4m_K^2 - m_\pi^2)$
$\eta \eta' \rightarrow \eta' \eta'$	$\frac{\sqrt{2}}{9f^2} (8m_K^2 - 5m_\pi^2)$
$\eta \eta' \rightarrow \eta' \eta_c$	0
$\eta' \eta' \rightarrow \eta' \eta'$	$-\frac{1}{9f^2} (16m_K^2 - 7m_\pi^2)$
$\eta' \eta' \rightarrow \eta' \eta_c$	0
$\eta' \eta_c \rightarrow \eta' \eta_c$	0

- [1] S. K. Choi *et al.* [Belle], Observation of a narrow charmonium-like state in exclusive $B^\pm \rightarrow K^\pm \pi^+ \pi^- J/\psi$ decays, Phys. Rev. Lett. **91** (2003), 262001.
- [2] R. L. Workman *et al.* [Particle Data Group], Review of Particle Physics, PTEP **2022** (2022), 083C01.
- [3] S. Pakvasa and M. Suzuki, On the hidden charm state at 3872 MeV, Phys. Lett. B **579** (2004), 67-73.
- [4] W. Chen, T. G. Steele, H. X. Chen and S. L. Zhu, Mass spectra of Z_c and Z_b exotic states as hadron molecules, Phys. Rev. D **92** (2015), 054002.
- [5] R. Molina and E. Oset, The $Y(3940)$, $Z(3930)$ and the $X(4160)$ as dynamically generated resonances from the vector-vector interaction, Phys. Rev. D **80** (2009), 114013.
- [6] F. K. Guo, C. Hanhart, U. G. Meißner, Q. Wang, Q. Zhao and B. S. Zou, Hadronic molecules, Rev. Mod. Phys. **90** (2018) no.1, 015004 [erratum: Rev. Mod. Phys. **94** (2022) no.2, 029901].
- [7] D. Gamermann, E. Oset, D. Strottman and M. J. Vicente Vacas, Dynamically generated open and hidden charm meson systems, Phys. Rev. D **76** (2007), 074016.
- [8] D. Gamermann, E. Oset and B. S. Zou, The radiative decay of $\psi(3770)$ into the predicted scalar state $X(3700)$, Eur. Phys. J. A **41** (2009), 85-91.
- [9] S. Prelovsek, S. Collins, D. Mohler, M. Padmanath and S. Piemonte, Charmonium-like resonances with $J^{PC} = 0^{++}, 2^{++}$ in coupled $D\bar{D}$, $D_s\bar{D}_s$ scattering on the lattice, JHEP **06** (2021), 035.
- [10] X. K. Dong, F. K. Guo and B. S. Zou, A survey of heavy-heavy hadronic molecules, Commun. Theor. Phys. **73** (2021), 125201.
- [11] H. X. Chen, Hadronic molecules in B decays, Phys. Rev. D **105** (2022), 094003.
- [12] P. P. Shi, Z. H. Zhang, F. K. Guo and Z. Yang, $D^+ D^-$ hadronic atom and its production in pp and $p\bar{p}$ collisions, Phys. Rev. D **105** (2022), 034024.
- [13] Q. Xin, Z. G. Wang and X. S. Yang, Analysis of the $X(3960)$ and related tetraquark molecular states via the QCD sum rules, AAPPs Bull. **32** (2022) 1, 37.
- [14] F. Z. Peng, M. J. Yan and M. Pavon Valderrama, Heavy- and light-flavor symmetry partners of the $T_{cc}^+(3875)$, the $X(3872)$ and the $X(3960)$ from light-meson exchange saturation, Phys. Rev. D **108** (2023), 114001.
- [15] H. Mutuk, Molecular interpretation of $X(3960)$ as $D_s^+ D_s^-$ state, Eur. Phys. J. C **82** (2022) no.12, 1142.
- [16] B. Wang, K. Chen, L. Meng and S. L. Zhu, Spectrum of the molecular tetraquarks: Unraveling the $T_{cs0}(2900)$ and $T_{cs0}^a(2900)$, Phys. Rev. D **109** (2024), 034027.
- [17] D. Gamermann and E. Oset, Hidden charm dynamically generated resonances and the $e^+ e^- \rightarrow J/\psi D\bar{D}$, $J/\psi D\bar{D}^*$ reactions, Eur. Phys. J. A **36** (2008), 189-194.
- [18] E. Wang, W. H. Liang and E. Oset, Analysis of the $e^+ e^- \rightarrow J/\psi D\bar{D}$ reaction close to the threshold concerning claims of a $\chi_{c0}(2P)$ state, Eur. Phys. J. A **57** (2021), 38.
- [19] K. Chilikin *et al.* [Belle], Observation of an alternative $\chi_{c0}(2P)$ candidate in $e^+ e^- \rightarrow J/\psi D\bar{D}$, Phys. Rev. D **95** (2017), 112003.

- [20] L. R. Dai, J. J. Xie and E. Oset, $B^0 \rightarrow D^0 \bar{D}^0 K^0$, $B^+ \rightarrow D^0 \bar{D}^0 K^+$, and the scalar $D\bar{D}$ bound state, *Eur. Phys. J. C* **76** (2016) 3, 121.
- [21] S. Uehara *et al.* [Belle], Observation of a χ'_{c2} candidate in $\gamma\gamma \rightarrow D\bar{D}$ production at BELLE, *Phys. Rev. Lett.* **96** (2006), 082003.
- [22] B. Aubert *et al.* [BaBar], Observation of the $\chi_{c2}(2P)$ meson in the reaction $\gamma\gamma \rightarrow D\bar{D}$ at BaBar, *Phys. Rev. D* **81** (2010), 092003.
- [23] O. Deineka, I. Danilkin and M. Vanderhaeghen, Dispersive analysis of the $\gamma\gamma \rightarrow D\bar{D}$ data and the confirmation of the $D\bar{D}$ bound state, *Phys. Lett. B* **827** (2022), 136982.
- [24] E. Wang, H. S. Li, W. H. Liang and E. Oset, Analysis of the $\gamma\gamma \rightarrow D\bar{D}$ reaction and the $D\bar{D}$ bound state, *Phys. Rev. D* **103** (2021), 054008.
- [25] C. W. Xiao and E. Oset, Three methods to detect the predicted $D\bar{D}$ scalar meson $X(3700)$, *Eur. Phys. J. A* **49** (2013), 52.
- [26] L. Dai, G. Toledo and E. Oset, Searching for a $D\bar{D}$ bound state with the $\psi(3770) \rightarrow \gamma D^0 \bar{D}^0$ decay, *Eur. Phys. J. C* **80** (2020) 6, 510.
- [27] L. L. Wei, H. S. Li, E. Wang, J. J. Xie, D. M. Li and Y. X. Li, Search for a $D\bar{D}$ bound state in the $\Lambda_b \rightarrow \Lambda D\bar{D}$ process, *Phys. Rev. D* **103** (2021), 114013.
- [28] P. C. S. Brandão, J. Song, L. M. Abreu and E. Oset, B^+ decay to $K^+ \eta\eta$ with $(\eta\eta)$ from the $D\bar{D}(3720)$ bound state, *Phys. Rev. D* **108** (2023), 054004.
- [29] M. Ablikim *et al.* [BESIII], Search for a scalar partner of the $X(3872)$ via $\psi(3770)$ decays into $\gamma\eta\eta'$ and $\gamma\pi^+\pi^- J/\psi$, *Phys. Rev. D* **108** (2023), 052012.
- [30] R. Aaij *et al.* [LHCb], [arXiv:2403.03586 [hep-ex]].
- [31] Z. P. Xing, F. Huang and W. Wang, Angular distributions for $\Lambda_b \rightarrow \Lambda_c^*(pK^-) J/\psi (\rightarrow \ell^+ \ell^-)$ decays, *Phys. Rev. D* **106** (2022), 114041.
- [32] M. Y. Duan, E. Wang and D. Y. Chen, Searching for the open flavor tetraquark $T_{c\bar{s}0}^{++}(2900)$ in the process $B^+ \rightarrow K^+ D^+ D^-$, [arXiv:2305.09436 [hep-ph]].
- [33] W. T. Lyu, Y. H. Lyu, M. Y. Duan, D. M. Li, D. Y. Chen and E. Wang, The roles of the $T_{c\bar{s}0}(2900)^0$ and $D_0^*(2300)$ in the process $B^- \rightarrow D_s^+ K^- \pi^-$, *Phys. Rev. D* **109** (2024), 014008.
- [34] W. H. Han, J. Xu and Y. Xing, The production of charmonium pentaquark from b -baryon and B -meson decay: SU(3) analysis, [arXiv:2310.17125 [hep-ph]].
- [35] F. Huang, Y. Xing and J. Xu, Searching for tetraquark through weak decays of b -baryons, *Eur. Phys. J. C* **82** (2022) no.11, 1075.
- [36] I. Bediaga and C. Göbel, Direct CP violation in beauty and charm hadron decays, *Prog. Part. Nucl. Phys.* **114**, 103808 (2020).
- [37] F. L. Wang, X. D. Yang, R. Chen and X. Liu, Correlation of the hidden-charm molecular tetraquarks and the charmoniumlike structures existing in the $B \rightarrow XYZ + K$ process, *Phys. Rev. D* **104** (2021), 094010.
- [38] L. R. Dai, G. Y. Wang, X. Chen, E. Wang, E. Oset and D. M. Li, The $B^+ \rightarrow J/\psi \omega K^+$ reaction and $D^* \bar{D}^*$ molecular states, *Eur. Phys. J. A* **55** (2019) no.3, 36.
- [39] Y. Zhang, E. Wang, D. M. Li and Y. X. Li, Search for the $D^* \bar{D}^*$ molecular state $Z_c(4000)$ in the reaction $B^- \rightarrow J/\psi \rho^0 K^-$, *Chin. Phys. C* **44** (2020) no.9, 093107.
- [40] E. Wang, J. J. Xie, L. S. Geng and E. Oset, Analysis of the $B^+ \rightarrow J/\psi \phi K^+$ data at low $J/\psi \phi$ invariant masses and the $X(4140)$ and $X(4160)$ resonances, *Phys. Rev. D* **97** (2018), 014017.
- [41] R. Aaij *et al.* [LHCb], Observation of New Resonances Decaying to $J/\psi K^+$ and $J/\psi \phi$, *Phys. Rev. Lett.* **127** (2021), 082001.
- [42] T. Aaltonen *et al.* [CDF], Evidence for a Narrow Near-Threshold Structure in the $J/\psi \phi$ Mass Spectrum in $B^+ \rightarrow J/\psi \phi K^+$ Decays, *Phys. Rev. Lett.* **102** (2009), 242002.
- [43] V. M. Abazov *et al.* [D0], Search for the $X(4140)$ state in $B^+ \rightarrow J/\psi \phi K^+$ decays with the D0 Detector, *Phys. Rev. D* **89** (2014), 012004.
- [44] R. Aaij *et al.* [LHCb], A model-independent study of resonant structure in $B^+ \rightarrow D^+ D^- K^+$ decays, *Phys. Rev. Lett.* **125** (2020), 242001.
- [45] R. Aaij *et al.* [LHCb], Amplitude analysis of the $B^+ \rightarrow D^+ D^- K^+$ decay, *Phys. Rev. D* **102** (2020), 112003.
- [46] A. Vinokurova *et al.* [Belle], Search for B decays to final states with the η_c meson, *JHEP* **06** (2015), 132 [erratum: *JHEP* **02** (2017), 088].
- [47] E. Kou *et al.* [Belle-II], The Belle II Physics Book, *PTEP* **2019** (2019), 123C01 [erratum: *PTEP* **2020** (2020), 029201].
- [48] V. Bhardwaj [Belle-II], Prospects in spectroscopy with Belle II, *Springer Proc. Phys.* **234** (2019), 181-187.
- [49] J. M. Xie, M. Z. Liu and L. S. Geng, Production rates of $D_s^+ D_s^-$ and $D\bar{D}$ molecules in B decays, *Phys. Rev. D* **107** (2023), 016003.
- [50] Z. Wang, Y. Y. Wang, E. Wang, D. M. Li and J. J. Xie, The scalar $f_0(500)$ and $f_0(980)$ resonances and vector mesons in the single Cabibbo-suppressed decays $\Lambda_c \rightarrow p K^+ K^-$ and $p \pi^+ \pi^-$, *Eur. Phys. J. C* **80** (2020) 9, 842.
- [51] J. Y. Wang, M. Y. Duan, G. Y. Wang, D. M. Li, L. J. Liu and E. Wang, The $a_0(980)$ and $f_0(980)$ in the process $D_s^+ \rightarrow K^+ K^- \pi^+$, *Phys. Lett. B* **821** (2021), 136617.
- [52] W. Y. Liu, W. Hao, G. Y. Wang, Y. Y. Wang, E. Wang and D. M. Li, Resonances $X(4140)$, $X(4160)$, and $P_{cs}(4459)$ in the decay of $\Lambda_b \rightarrow J/\psi \Lambda \phi$, *Phys. Rev. D* **103** (2021), 034019.
- [53] M. Y. Duan, J. Y. Wang, G. Y. Wang, E. Wang and D. M. Li, Role of scalar $a_0(980)$ in the single Cabibbo suppressed process $D^+ \rightarrow \pi^+ \pi^0 \eta$, *Eur. Phys. J. C* **80** (2020) 11, 1041.
- [54] H. Zhang, Y. H. Lyu, L. J. Liu and E. Wang, Role of the scalar $f_0(980)$ in the process $D_s^+ \rightarrow \pi^+ \pi^0 \pi^0$, *Chin. Phys. C* **47** (2023) no.4, 043101.
- [55] X. C. Feng, L. L. Wei, M. Y. Duan, E. Wang and D. M. Li, The $a_0(980)$ in the single Cabibbo-suppressed process $\Lambda_c \rightarrow \pi^0 \eta p$, *Phys. Lett. B* **846** (2023), 138185.
- [56] R. Aaij *et al.* [LHCb], Observation of a resonant structure near the $D_s^+ D_s^-$ threshold in the $B^+ \rightarrow D_s^+ D_s^- K^+$ decay, *Phys. Rev. Lett.* **131** (2023), 071901.
- [57] M. Bayar, A. Feijoo and E. Oset, $X(3960)$ seen in $D_s^+ D_s^-$ as the $X(3930)$ state seen in $D^+ D^-$, *Phys. Rev. D* **107** (2023), 034007.
- [58] D. Guo, J. Z. Wang, D. Y. Chen and X. Liu, Connection between near the $D_s^+ D_s^-$ threshold enhancement in $B^+ \rightarrow D_s^+ D_s^- K^+$ and conventional charmonium $\chi_{c0}(2P)$, *Phys. Rev. D* **106** (2022), 094037.
- [59] Z. m. Ding and J. He, Combined analysis on nature of $X(3960)$, $\chi_{c0}(3930)$, and $X_0(4140)$, *Eur. Phys. J. C* **83** (2023) no.9, 806.
- [60] X. Liu, H. Huang, J. Ping, D. Chen and X. Zhu, The explanation of some exotic states in the $c\bar{s}\bar{s}$ tetraquark system, *Eur. Phys. J. C* **81** (2021) no.10, 950.

- [61] J. Lu, X. Luo, M. Song and G. Li, Pole determination of $X(3960)$ and $X_0(4140)$ in decay $B^+ \rightarrow K^+ D_s^+ D_s^-$, [arXiv:2312.02454 [hep-ph]].
- [62] J. J. Qi, Z. Y. Wang, Z. F. Zhang and X. H. Guo, The properties of the S -wave $D_s \bar{D}_s$ bound state, [arXiv:2308.07704 [hep-ph]].
- [63] S. Y. Li, Y. R. Liu, Z. L. Man, Z. G. Si and J. Wu, The $X(3960)$, $X_0(4140)$, and other $cs\bar{c}s$ compact states, [arXiv:2308.06768 [hep-ph]].
- [64] Y. Chen, H. Chen, C. Meng, H. R. Qi and H. Q. Zheng, On the nature of $X(3960)$, Eur. Phys. J. C **83** (2023) no.5, 381.
- [65] A. Ali, G. Kramer and C. D. Lu, Experimental tests of factorization in charmless nonleptonic two-body B decays, Phys. Rev. D **58**, 094009 (1998).